

EXPERIMENTAL AND THEORETICAL ANALYSIS OF SURGE IN THE CENTRIFUGAL COMPRESSOR

Dr.abdulkareem a. wahab albehigi
Email: abdulcareemwahab78@yahoo.com

rasha hayder hashim
Email: rashalkayat@yahoo.com

ABSTRACT

Surge is an unstable operating mode of compression systems which occurs at low mass flow where the pressure delivered by the compressor is less than the plenum pressure. This instability is global, one- dimensional and nonlinear. It is characterized by a limit-cycle oscillation in mass flow and pressure rise.

This paper presented application of active surge control in centrifugal compressor, with measurement and evaluation of the thermodynamic operational parameters of the compressor system. In experimental work investigation the surge phenomenon by measuring and calculating mass flow rate and outlet pressure from sensors and manometers and designing plenum to move the surge line to the left side of the compressor map. The variable speed compressor characteristic is derived based on energy losses in a compressor components. Active control of surge in connection with varying speed is studied.

KEYWORDS: compressor, surge, plenum, losses, pressure rise, mass flow

الخلاصة :-

ظاهرة الجيشان هي شكل غير مسبق لعمل منظومة الضاغط تحدث عند تصريف كتلة قليلة عندما يكون الضغط الخارج من الضاغط أقل من ضغط المنظومة. هذه الظاهرة تكون شاملة وفي اتجاه واحد وغير خطية وهي توصف بحدود تذبذبات دورية في كتلة الانسياب وارتفاع الضغط .

هذا البحث هو تطبيق لسيطرة مؤثرة للجيشان في ضاغط نابذة مع قياسات وتقييم للمعطيات الترموديناميكية لعملية منظومة الضغط. في الجانب العملي تم التحقق من ظاهرة الجيشان عن طريق حساب معدل تدفق الجريان والضغط الخارج بواسطة السنسرات والمانوميترات وتم تصميم خزان لتحريك خط الجيشان. مواصفات تغير سرعة الضاغط اشتقت على أساس الخسائر في الطاقة لمكونات الضاغط، كما درست السيطرة المؤثرة على الجيشان المرتبطة مع تغير السرعة.

الكلمات المحكمة: الضاغط ، الجيشان ، الخزان ، الخسائر ، ارتفاع الضغط ، الانسياب الكتلي

INTRODUCTION

Compressors are machines compress the air or gas. Applications involve air compression for use in air craft engines, in industrial gas turbines and in turbocharged combustion engines.

In a typical centrifugal compressor the fluid is forced through the impeller by rapidly rotating impeller blades. The velocity of the fluid is converted to pressure partially in the impeller and partially in the volute or in the stationary diffusers. Most of the velocity leaving the impeller is converted into pressure energy in the volute or in the diffuser.

[N. Chaoqun, *et al.*2000], analyzed the dynamic behavior of surge in the actual centrifugal compression system by experimental study. The surge phenomenon was suppressed and the stable operating range of the system was extended. The experimental results showed that the length of the time which the compression system enters surge compulsively was shorter than the time for spontaneous surge. The strength of the surge was positively proportional to the B parameters, the frequency of surge was negatively proportional to the B parameter, (B parameter = $\frac{U_t}{2\omega_H L_c}$, where U_t is the tip speed of the compressor blade, ω_H is the Helmholtz frequency and L_c is the length of the duct). The results reveal that the inception of surge can be diagnosed at both the outlet of the centrifugal fan and the plenum and the stable range where the actual centrifugal compression system operated was extended by 24% with the technique of the active control.

[J. Gravdahl, *et al.*2004], presented the derivation of a compressor characteristic, and the experimental validation of a dynamic model for a variable speed centrifugal compressor, a variable speed compressor characteristic was derived by used energy transfer and loss analysis. The model was based on the underlying physics of the system and required only a few parameters to be estimated from experimental data. It was demonstrated that taking into account the loss due to friction, incidence, mixing, and blade loading results in compressor characteristics that closely match the measured characteristics. The compressor consisted of a single-stage and number of impeller blades used was 20 with diameters 106 mm and 54 mm at inlet tip and inlet hub respectively, and the exit diameter 180 mm. It was operated at speed varying between (N= 16,000 and 22,000) rpm. The simulated response of the dynamic model was found to be in excellent agreement with the experimental results and good agreement of the experimental results leads to believe that the various losses for this compressor have been accurately modeled.

CENTRIFUGAL COMPRESSOR STAGE :-

Every compressor stage consists of several basic parts. Schematic sketch of common used flow compressor is given in figure (1), in inlet casing of compressor (0-1) the fluid is accelerated and the static pressure falls from P_0 to P_1 and then goes to impeller (1-2), where its velocity is due to centrifugal forces increases, at the same time pressure of gas is also increased. Then the gas flows into diffuser (2-3) where part of its kinetic energy is changed to pressure energy.

A centrifugal compressor consists essentially of a rotating impeller followed by diffuser and the collector (volute). Figure (2) shows diagrammatically the various elements of a centrifugal compressor. Both the static pressure and the velocity are increased within the impeller. Impeller can be single or double – entry type, depending on the pressure rise and flow rate needed. The fluid will then enter a diffuser, where the velocity is decreased. The purpose of the diffuser is to convert the kinetic energy of the fluid leaving the impeller into pressure energy. The hub is the curved surface of revolution of the impeller a – b, the shroud is curved surface c – d, [S. Dixon 1998]. Figure (2) represent also the velocity triangle at impeller entry and exit where C represents the absolute velocity of air, U represent impeller tip speed and W represent relative velocity of air. Absolute velocity of air C has two components, tangential component C_θ and radial component C_r . The flow entering a centrifugal compressor in axial direction, this

is due to no tangential component velocity at entry of compressor, due to absence of inlet guide vanes that is meaning (α_1 is 90°) and (C_{o1} is zero), [A. Mironer 1979].

BASIC SURGE CONCEPTS :-

Surge is unstable operation mode of centrifugal compressors, which occurs when the operating point of the compressor is located to left of the surge line, which is the stability limit in the compressor map. The phenomenon is manifested as oscillations of the mass flow, pressure rise and rotational speed of the compressor. Surge is highly undesired and can cause severe damage to the machine. Traditionally, surge has been avoided using a surge avoidance scheme. Such schemes use various measures to keep the operating point of the compressor away from the surge line. Typically, a surge control line is drawn at distance from the surge line, and the surge avoidance scheme ensures that the operating point does not cross this line. This method restricts the operating range of the machine and efficiency is limited. Active surge control is fundamentally different to surge avoidance in that the unstable phenomenon is sought to be stabilized instead of avoided, [J. Gravdahl 2001].

Surge can be further defined according to the amplitude of the oscillations. Mild surge refers to small amplitude oscillation with a frequency near the Helmholtz resonator frequency. Classic surge is nonlinear phenomenon with larger oscillations and a lower frequency than mild surge but the mass flow fluctuations remain positive. Deep surge is most severe of these types, as reversed mass flow can occur in the compressor. This type of oscillation can cause reduced performance and efficiency of the compressor and even in some cases failure due to large unsteady aerodynamic force on blades, [D. Gysling 1989].

SURGE CONTROL :-

It is seen that the surge can lead to failure of the system due to large mechanical loads in the blading. Furthermore, these instabilities restrict the machines performance and efficiency. There are several methods for surge avoidance exists and active surge control and examples include recycle, bleed and throttle valves, gas injection, variable guide vanes and a number of others. The most widely used method in industrial compressor systems today is to use a recycle valve to divert gas from the compressor outlet and back to the inlet. This is to keep the flow through the compressor above the critical limit. The major drawback of the recycle valve is that the gas is run through the same compressor several times. This increases the energy consumption of the compressor. This solution has proved reliable, but is somewhat inefficient. Active surge control is a popular research field. The purpose of active surge control is to stabilize the compressor when operating within the unstable region of the compressor map. This is achieved by extending the stable operating envelope of the compressor, [T. Grong 2009].

Surge control techniques have been extensively explored. The main advantages of these techniques are their applicability to a wide range of machines and their considerable performance improvement compared to other techniques. Moreover, these techniques can be easily added to existing machines. Traditionally, the surge problem was tackled by using surge avoidance techniques. However, these techniques limit the operational range and reduce the efficiency of the compression system. Therefore, active surge control has been introduced as an alternative approach to suppressing surge rather than avoiding it, [R. Shehata 2009].

EXPERIMENTAL WORK :-

The main purpose of the experimental work detection the surge by measuring mass flow and pressure and noted when occurs positive curve between them the surge is begin. Secondly control the surge by move the surge line towards the left side. In section one of this works the

mass flow rate was measured from water manometer and the pressure were measured from (1) mercury manometers, (2) sensors, and plotted them (mass flow rate and delivery pressure) in four rotational speeds (21000, 23000, 25000 and 27000) rpm. Also calculated and plotted isentropic efficiencies in each speed by measuring temperatures at inlet and outlet and then plotted the efficiency with delivery pressure. Section two represented designing plenum and connected to the system by piping and valves to move the surge point towards the left side. Figure (3) shows the schematic diagram of the experimental test rig with plenum [R.Hashim 2013].

The compressor used in this study is a single – stage centrifugal compressor. This compressor test rig production from PLINT & PARTNERS LTD and its type VS – 57, from Paxton product. The compressor consists of:

1. Impeller: The impeller has 10 blades and rotates in high speed between (21000 – 29000). The outlet tip diameter is 145 mm and inlet tip diameter is 65 mm.
2. Volute: The volute surrounding the impeller and use to convert the kinetic energy into static pressure by gradual expansion. The maximum diameter of the volute is 260 mm and the thickness of tongue is 2.85 mm. Figure (4) shows the volute with impeller.

Experimental Procedure of Operation and Testing :-

1. The centrifugal compressor was provided with electric power and allowed to reach steady state. At the beginning the throttle valve at outlet pipe should be closed a few seconds to start up load on the planetary drive and make vacuum inside the body of the compressor, then start gradually open to allow air enter to the compressor.
2. The impeller was run at high rotational speeds between (21000 to 29000) rpm. This speed is changed by handles put on the base. In this study, four rotational speeds (21000, 23000, 25000 and 27000) rpm were used.
3. The flow rate was controlled by the throttle valve on the outlet pipe. This valve is graduated into ten readings. In this study seven reading (10, 20, 30, 40, 60, 80, and 100) % from open throttle valve were used.
4. The manometers were read indicating different heads in each change degree opening of throttle valve. The water manometer read the stagnation head, the first mercury manometer read the suction head and the second mercury manometer read the delivery head. From these heads of manometers different pressures are calculated.
5. Comparison the manometers with sensors and then used these sensors to measure the pressures. The number of samples were collected by the data logger and read every second. The total time of each test about 30 seconds and the average of these 30 reading were calculated for each test.
6. The plenum designed in dimensions (diameter = 57 mm and length = 900 mm) to control the surge. This plenum connected with outlet pipe of the compressor by pipes.
7. Returned read the pressures from sensors and plotted with mass flow rate in the same rotational speeds used at the beginning and compared these results with the result obtained from the system before connecting with plenum.

THEORETICAL ANALYSIS :-

Study a mathematical analysis of the compressor characteristic for a variable speed compressor. The dynamic model used based on the thermo – and fluid mechanics processes taking place in a centrifugal compressor. The energy losses in the compressor components is used to derive the characteristic, fluid friction and incidence losses, as well as other losses, in the compressor components are modeled, and a variable speed compressor characteristic is

developed based on this analysis. The physical model considered in this study is shown in figure (5) which represents compression system with close coupled valve [J. Gravdahl 1998]. A compression system consisting of a centrifugal compressor, closed coupled valve (CCV), compressor duct, plenum volume and a throttle. The calculation of the compressor pressure rise will be based on energy transfer and energy losses in the various parts of the compressor.

Governing Equations

The governing equations of the fluid flow are derived and applied as follows,[Gravdahl 1998].

$$\text{Isentropic Efficiency} = \frac{\Delta h_{ideal}}{\Delta h_{actual}} = \frac{h_{2s} - h_{01}}{h_{02} - h_{01}} \quad (1)$$

$$\text{From perfect gas } h = C_p \times T \quad (2)$$

Inserting equation (2) in (1) yields:

$$\text{isentropic efficiency} = \frac{C_p T_{01} \left(\frac{T_{2s}}{T_{01}} - 1 \right)}{C_p (T_{02} - T_{01})} \quad (3)$$

From equation of state:

$$PV^\gamma = \text{Constant} \quad (4)$$

And equation of the perfect gas:

$$PV = mRT \quad (5)$$

We obtained:

$$\frac{T_2}{T_1} = \left(\frac{P_2}{P_1} \right)^{\frac{\gamma-1}{\gamma}} \quad (6)$$

Inserting (6) in (3)

$$\Rightarrow \text{isentropic efficiency} = \frac{C_p T_{01} \left[\left(\frac{P_2}{P_{01}} \right)^{\frac{\gamma-1}{\gamma}} - 1 \right]}{C_p [T_{02} - T_{01}]} \quad (7)$$

$$\text{But } C_p (T_{02} - T_{01}) = \Delta h_{0c,ideal} \quad (8)$$

$$\therefore \text{isentropic efficiency} = \frac{C_p T_{01} \left[\left(\frac{P_2}{P_{01}} \right)^{\frac{\gamma-1}{\gamma}} - 1 \right]}{\Delta h_{0c,ideal}} \quad (9)$$

From equation (9) obtain the outlet pressure

$$P_2 = \left[1 + \frac{\eta_{is} \times \Delta h_{0c,ideal}}{C_p T_{01}} \right]^{\frac{\gamma}{\gamma-1}} \times P_{01} \quad (10)$$

Equation (10) used in to determine the outlet pressure from compressor. To calculate outlet pressure from equation (10) η_{is} and $\Delta h_{0c,ideal}$ must be calculated [J. Gravdahl 1998].

$$\Delta h_{0c,ideal} = U_2 C_{02} \quad (11)$$

$$\text{slip factor } (\sigma) = \frac{C_{02}}{U_2} \Rightarrow C_{02} = \sigma U_2 \quad (12)$$

Inserting equation (12) in (11) yields:

$$\Delta h_{0c,ideal} = \sigma U_2^2 \quad (13)$$

$$\text{The slip factor is define as } \sigma \cong 1 - \frac{2}{i} \quad (14)$$

The approximation is known as Stanitz formula, where i is the number of impeller blades, the slip factor σ varies between 0 and 1.

To calculate the isentropic efficiency of the compressor applies the following definition, [N. Cumpsty 1989]:

$$\eta_i(m, U_1) = \frac{\Delta h_{0c,ideal}}{\Delta h_{0c,ideal} + \Delta h_{loss}} - \Delta n \quad (15)$$

Δh_{loss} term is the summation of the friction losses and incidence losses in impeller and diffuser respectively and Δn is term to the summation of another losses that low effect.

$$(\Delta h_{loss} = \Delta h_{if} + \Delta h_{ii} + \Delta h_{df} + \Delta h_{di}) \quad (16)$$

According to [T. Ferguson 1963]:

$$\Delta h_{if} = \frac{C_h l}{2D \rho_{01}^2 A_1^2 \sin^2 \beta_{1b}} m^2 \quad (17)$$

From [J. Gravdahl 1998].

$$\Delta h_{ii} = \frac{1}{2} \left(U_1 - \frac{\cot \beta_{1b} m}{\rho_{01} A_1} \right)^2 \quad (18)$$

Δh_{if} , Δh_{ii} are friction losses in impeller, and incidence losses in the impeller respectively.

In the present model and equations, it is required to calculate the outlet pressure from different rotational speeds and in different percentage open throttle valve. To calculate the outlet pressure used the incidence losses Δh_{ii} instead of total losses to show the surge area. These values of the total pressure measuring in four different rotational speeds (21000 , 23000 , 25000 , 27000)rpm and in seven percentage open throttle valve (10 , 20 , 30 ,40 , 50 , 60 , 80 and 100)% .

RESULTS AND DISCUSSION :-

Figures (6-14) represent results calculating from experimental work

Figure (6) represents compressor characteristic curve, which is also called a compressor map, this curve shows the relationship between the mass flow rate and delivery pressure obtained from manometers in four rotational speeds (21000, 23000, 25000 and 27000) rpm. In this figure notice that when the rotational speed increase the mass flow rate and delivery pressure increase at the same degree opening of throttle valve and in this figure can be seen that the delivery pressure magnitudes produced by impeller are generally increase when the mass flow rate decrease in negative slop curve according to characteristic of the centrifugal flow compressor until reach to the surge point (maximum delivery pressure) after this point the delivery pressure decrease with decrease mass flow rate in positive curve. This area becomes unstable for a constant rotational speed. The surge point occurs when throttle valve opening at 30%. Figure (7) represent relationship between mass flow rate, delivery pressure and isentropic efficiency at rotational speed 23000rpm. The x-axis represents mass flow rate in kg/s, y-axis at the left side represents delivery pressure in kpa and the y-axis at the right side represents the isentropic efficiency. In this figure delivery pressure and isentropic efficiency increase when the mass flow rate decrease until reach to the surge point, in the left side of surge point the delivery pressure and isentropic efficiency decrease, this is due to reduce performance of the compressor. Figure (8) represents mass flow rate versus delivery pressure at speed 21000 rpm. In this figure maximum delivery pressure from sensors without plenum reach to 118 kpa at mass flow equal to 0.13 this is occurs at 30% open throttle valve while maximum delivery pressure obtain from sensors with plenum about 118.38 at mass flow rate about 0.074 kg/s this happened at 20% open throttle valve.

Figure (9) represents mass flow rate versus delivery pressure at speed 23000 rpm. In this figure maximum delivery pressure from sensors without plenum is 121.08 kpa at mass flow equal to 0.1307 this is occurs at 30% open throttle valve while maximum delivery pressure obtain from sensors with plenum about 121.27 at mass flow rate about 0.0826 kg/s this happened at 20% open throttle valve.

Figures (10) and (11) represent the compressor map with surge line from sensors before and after connect the plenum respectively. These curves show the relationship between the mass flow rate and delivery pressures obtain from sensors before and after connect the plenum to the compressor and these curves obtain by using four rotational speeds (21000, 23000, 25000 and

27000) rpm. In figure (10) the surge line occurs at 30% opening of throttle valve while in figure (11) the surge line occurs at 20% opening of throttle valve this mean that using the plenum moved the surge line about 10%.

Figure (12) represents the oscillation of the delivery pressure with the time at (30%) opening of throttle valve. This figure draw by using reading sensors before connects the compressor to the plenum. In this figure the fluctuations occur in pressure is high when the surge is start.

Figure (13) represents the oscillation of the delivery pressure with the time at (30%) opening of throttle valve. This figure draw by using reading sensors after connects the compressor to the plenum. In this figure the fluctuations in pressure is small because the surge is not start yet.

Figure (14) represents mass flow rate versus plenum pressure in speeds (21000, 25000 and 27000) rpm in this figure the plenum pressure increase with increase value of mass flow rate at constant rotational speed because the increase in mass flow rate due to increase in flow accumulated in plenum and this due to increase in pressure inside the plenum.

Figure (15) represents compressor map with surge line without plenum. These curves shows the relationship between mass flow rate and outlet pressures obtains from calculating before connecting the compressor to the plenum in four rotational speeds.

Figure (16) represents the compressor map with surge line with plenum. These curves show the relationship between mass flow rate and outlet pressures obtain from calculating after connecting the compressor with plenum in four different speeds.

Figures (17) and (18) represent the comparison between outlet pressures and mass flow rates calculating from experimental and theoretical works with and without plenum at speeds(21000 and 25000)rpm. In these figures the values of outlet pressure calculating from theoretical work larger than the values of outlet pressures measuring from experimental work because there are some losses neglected in theoretical calculation while took account in experimental calculation.

Figures (19) and (20) represent the comparison between results of this work and results from [Gravdahl et. al. 2000].Figure (19) represents the relationship between mass flow rate and outlet pressure calculating and measuring theoretically and experimentally in three speeds 21000 rpm, 23000 rpm, and 25000 rpm. Figure (20) represents the relationship between mass flow rate and pressure ratio calculating and measuring theoretically and experimentally from [Gravdahl et. al. 2000] in three rotational speeds, 18000 rpm, 21000 rpm and 23000 rpm. In these figures the curves represent the theoretical results upper than the curves represent the experimental results

CONCLUSIONS:-

1. It has been found that the surge phenomenon appeared in low mass flow rate when the throttle valve open at (10, 20, and 30) percentages open.
2. It has been found after connecting the plenum the surge area decrease and the surge line moved towards the left side of the compressor map.
3. The energy transfer equations and energy losses equations have been adopted in this research showed that the fluctuation in outlet pressures calculated from different type of losses (frictional losses and incidence losses) and another loss.
4. The positive curve of the relationship between the mass flow rate and outlet pressure occur because the incidence losses.
5. The pressures calculated from theoretical work is larger than the pressures calculated from experimental work, this occur because there are some losses neglected in theoretical part while effect in experimental part.

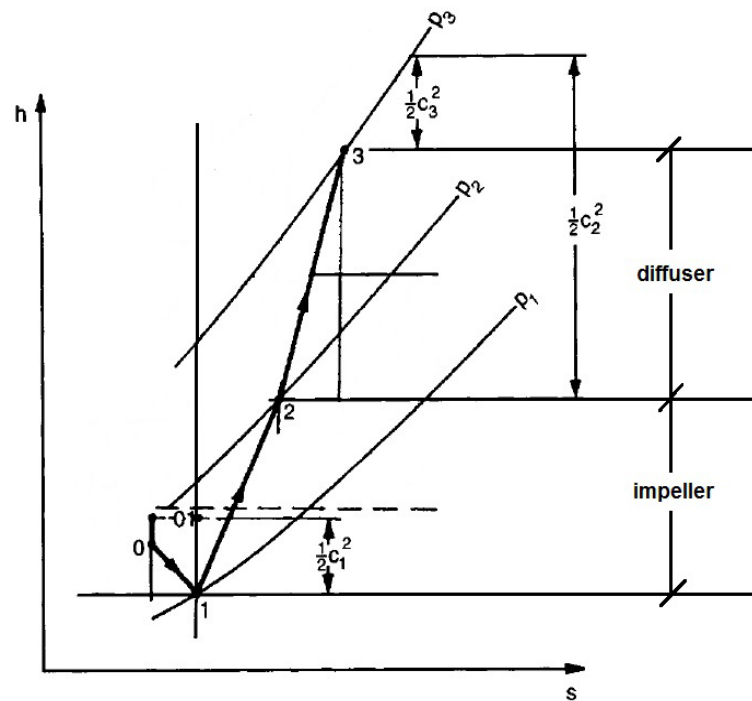


Figure (1) Diagram for the complete centrifugal compressor stage. [S. Dixon 1998].

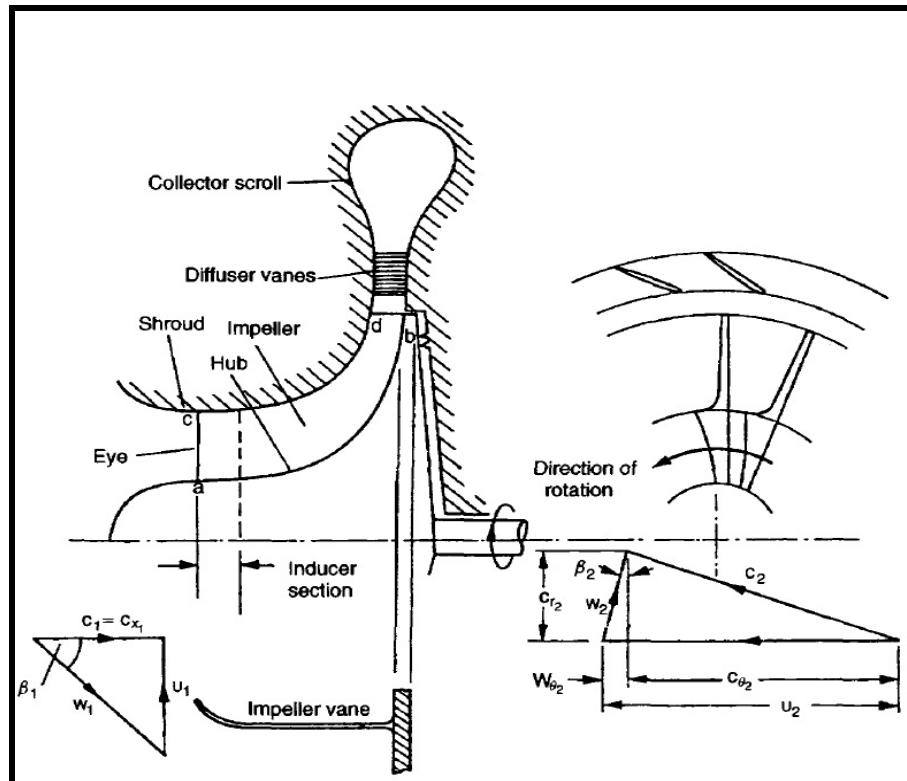


Figure (2) Centrifugal compressor stage and velocity diagrams.[S. Dixon 1998].

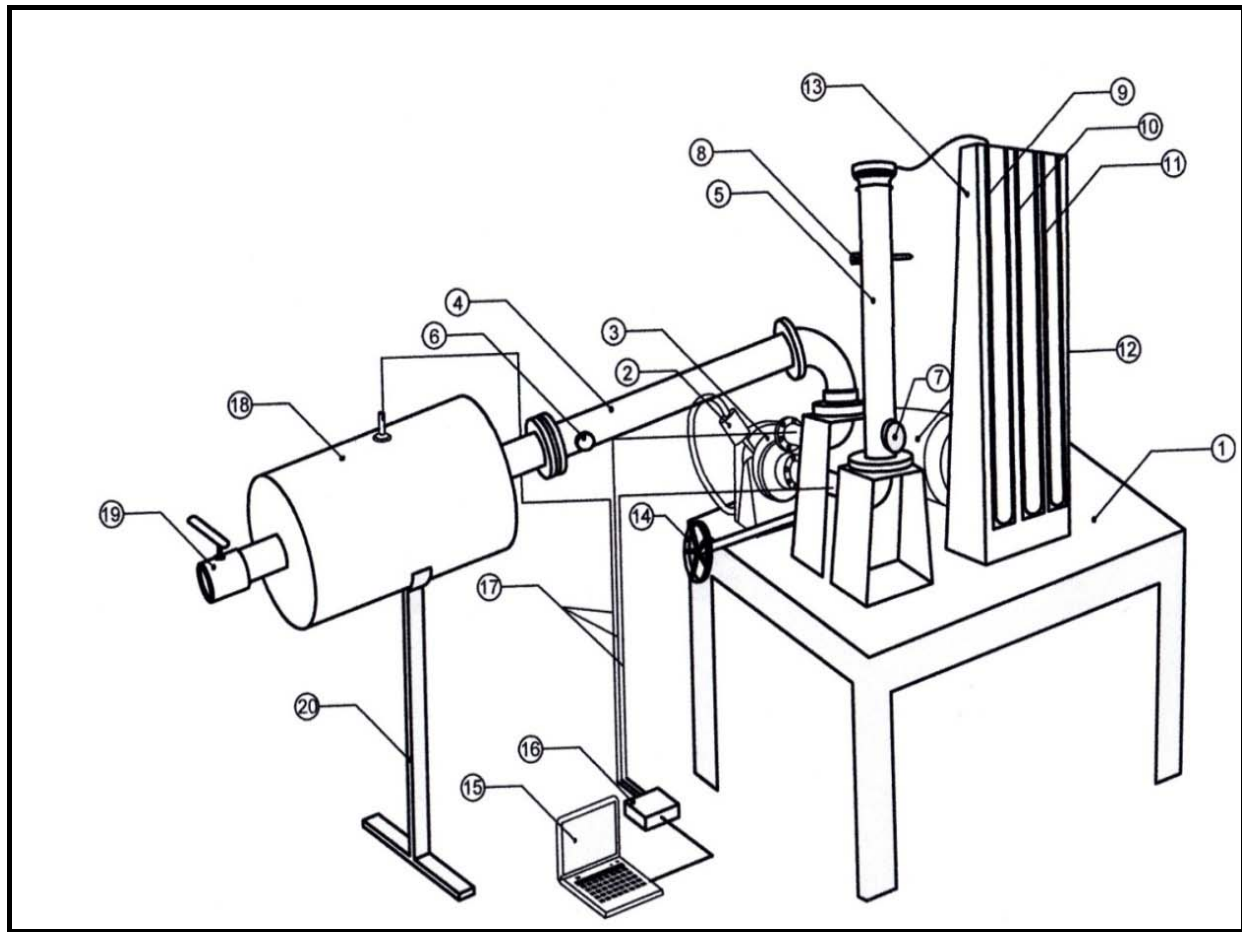


Figure (3) Schematic diagram of the experimental rig with plenum.[R. Hashim].

1	Base	11	Mercury manometer No 2
2	Oil container	12	Electrical motor
3	Centrifugal compressor	13	Box power
4	Outlet pipe	14	Handle for change speed
5	Inlet pipe	15	Personal computer
6	Throttle valve	16	Data logger
7	Inlet valve	17	Pressure transducers
8	Thermometer	18	Plenum
9	Water manometer	19	Valve
10	Mercury manometer No 1	20	Stand



Figure (4) Impeller and volute of centrifugal compressor.[R. Hashim].

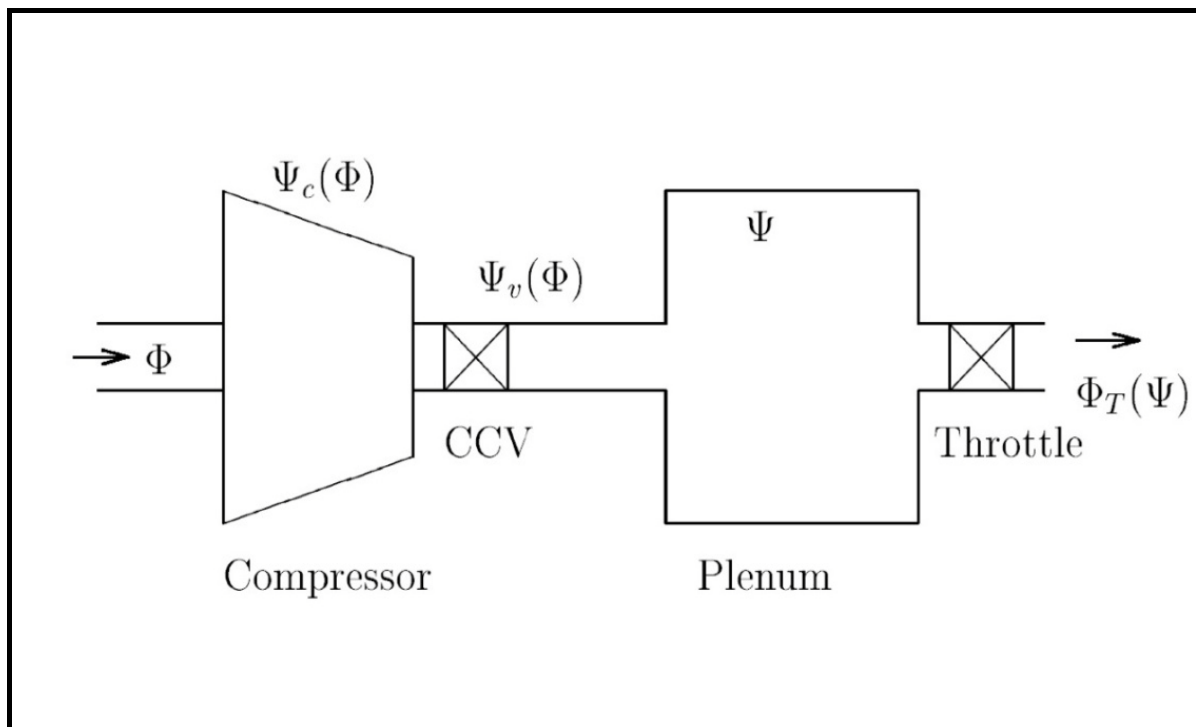


Figure (5) Centrifugal compression system with CCV [J. Gravdahl 1998].

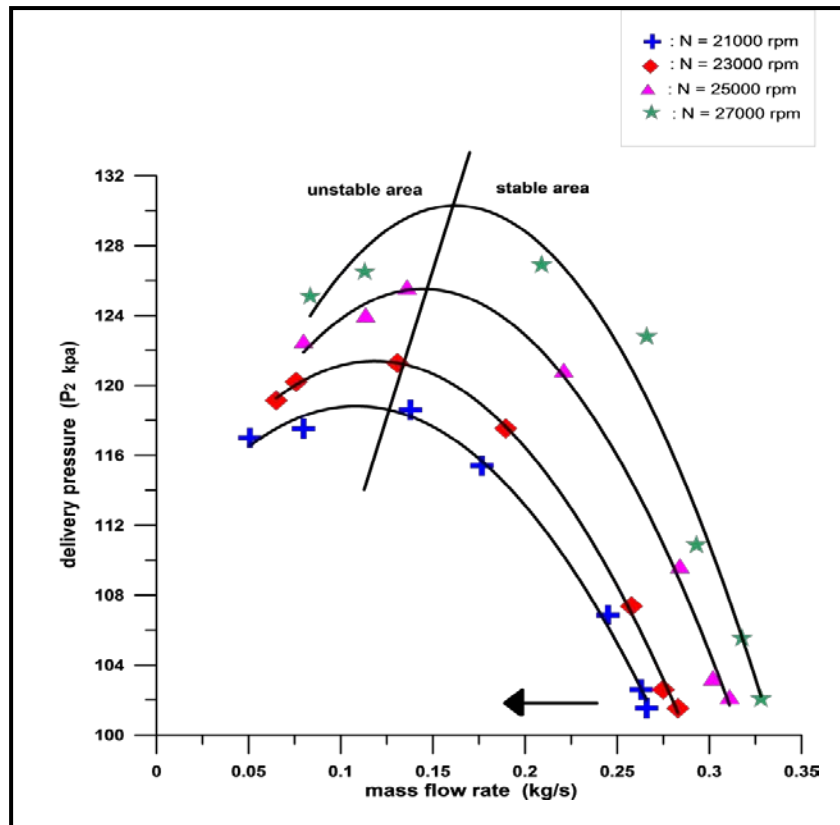


Figure (6) Mass flow rate versus delivery pressure from manometers at four rotational speeds.

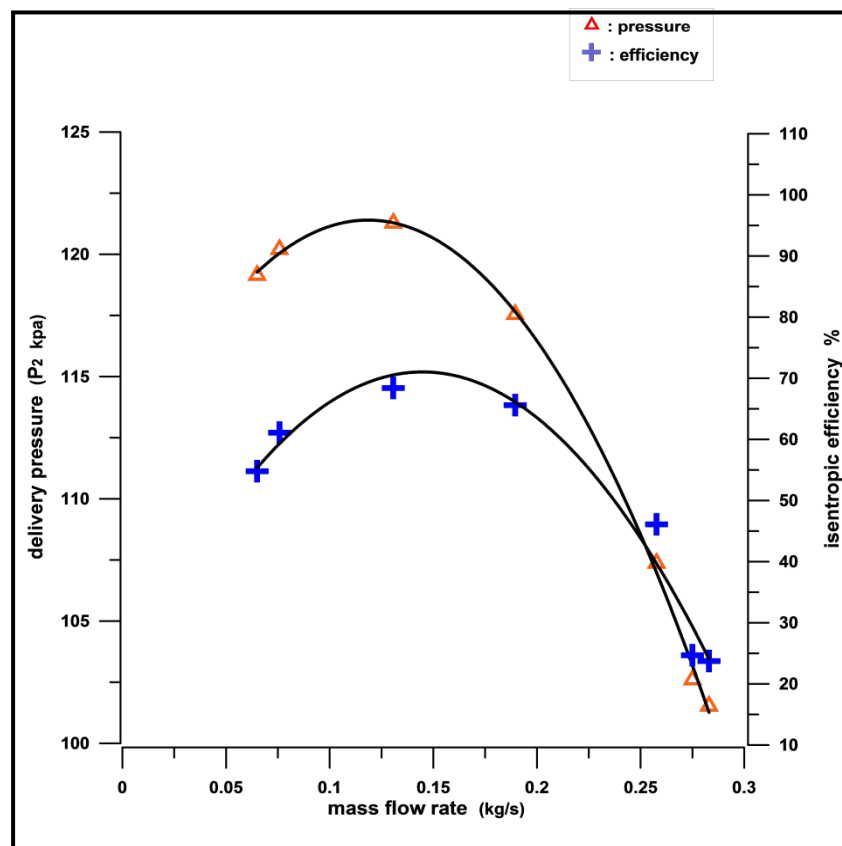


Figure (7) Mass flow rate, delivery pressure and isentropic efficiency from manometers at N=23000 rpm

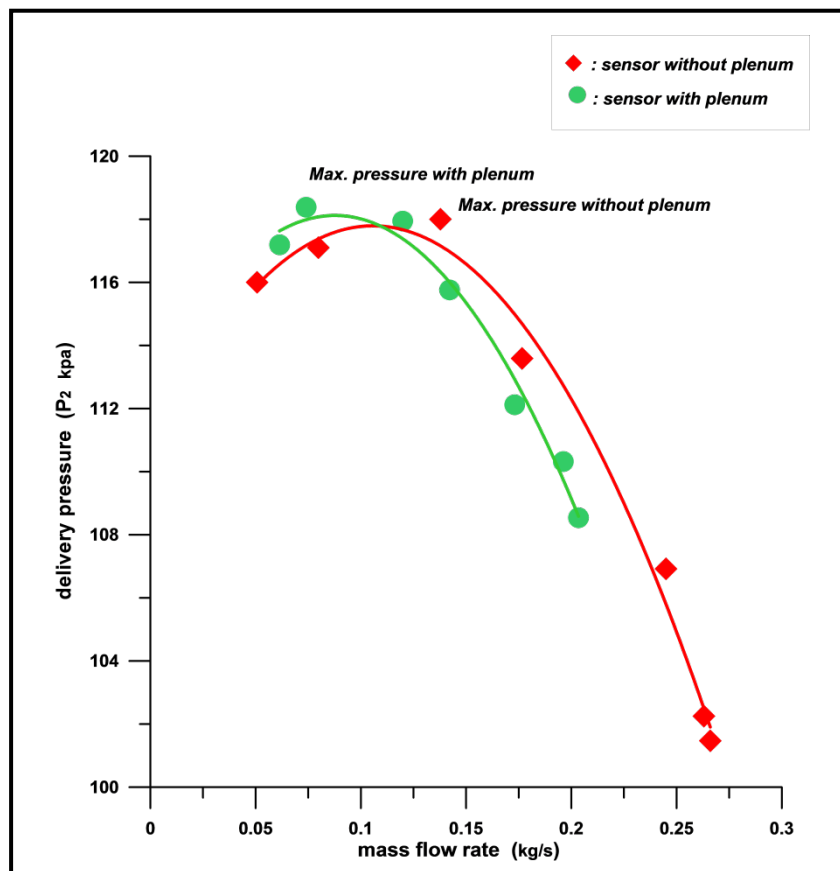


Figure (8) Mass flow rate versus delivery pressure by using sensors with and without plenum at N=21000 rpm.

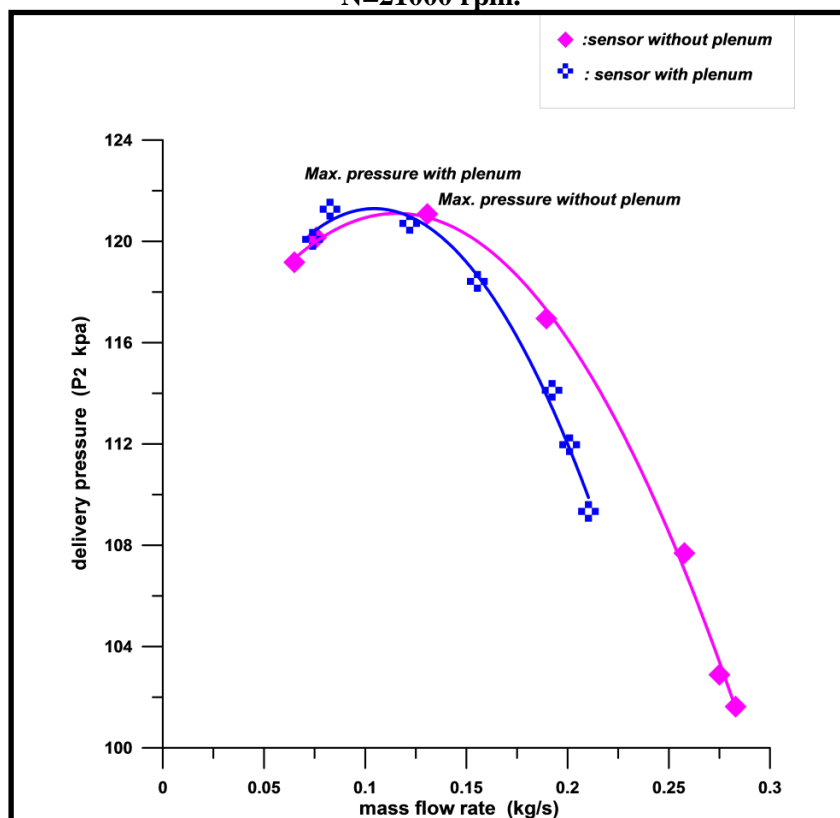


Figure (9) Mass flow rate versus delivery pressure by using sensors with and without plenum at N=23000 rpm.

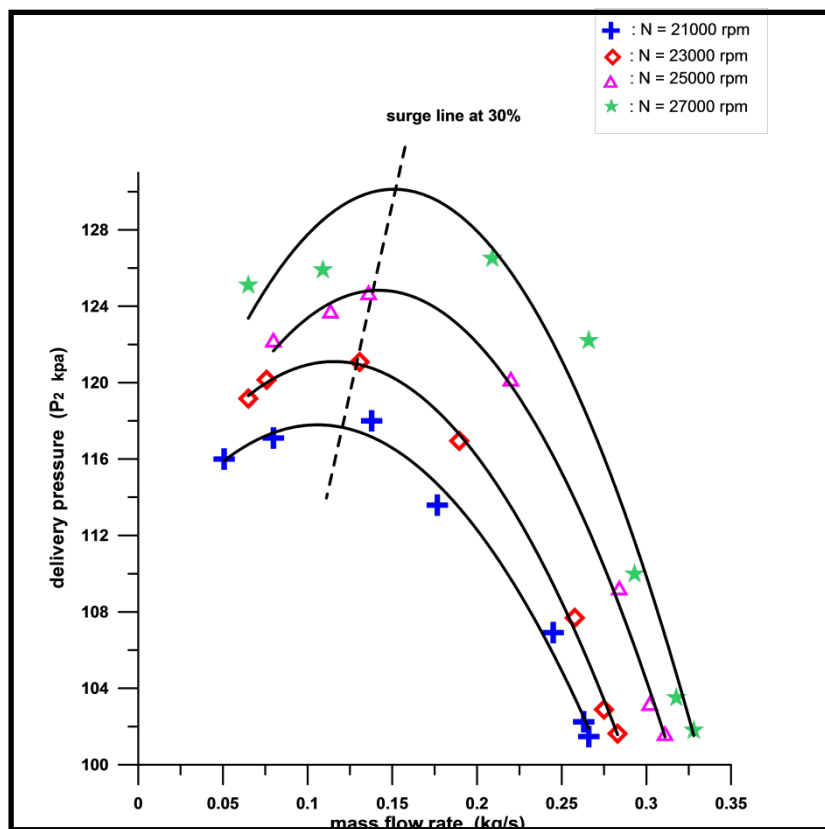


Figure (10) Mass flow rate versus delivery pressure from sensors without plenum at four rotational speeds with surge line.

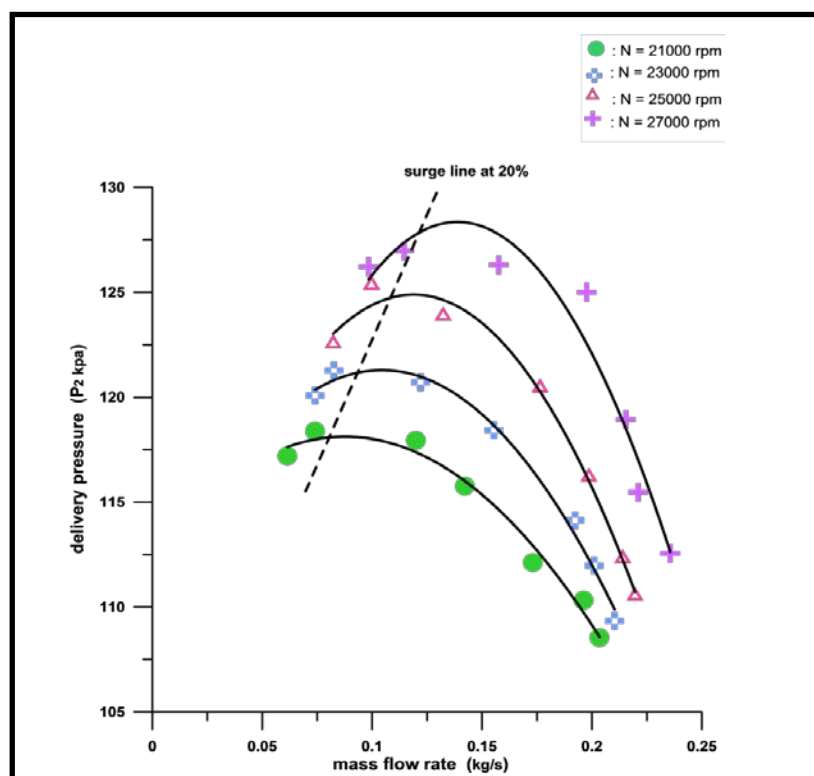


Figure (11) Mass flow rate versus delivery pressure from sensors with plenum at four rotational speeds with surge line.

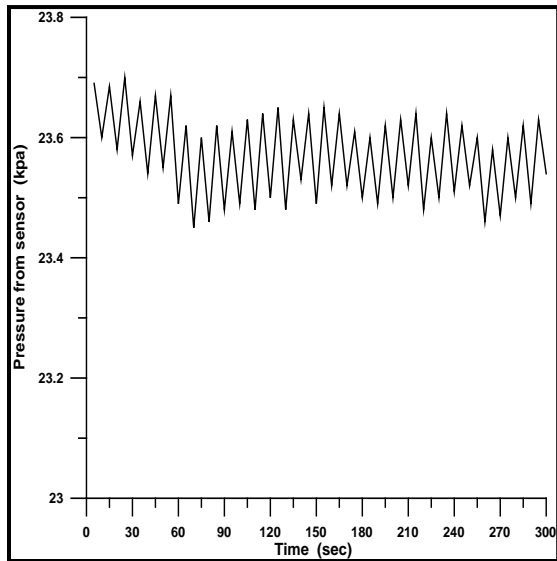


Figure (12) Time and pressure at 30% open throttle valve without plenum at 25000 rpm

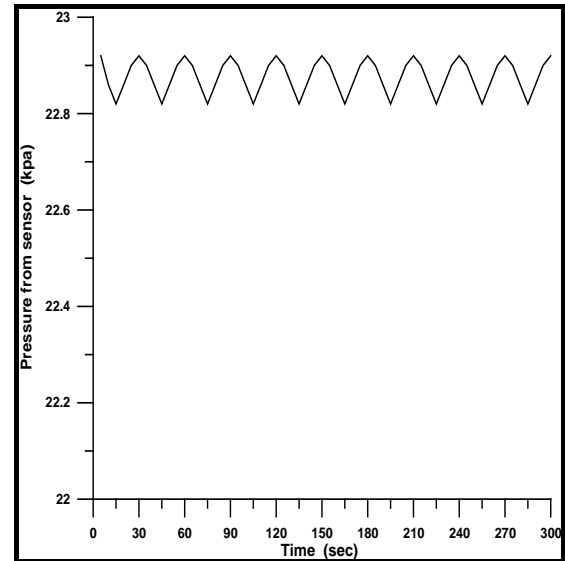


Figure (13) Time and pressure at 30% open throttle valve with plenum at 25000 rpm

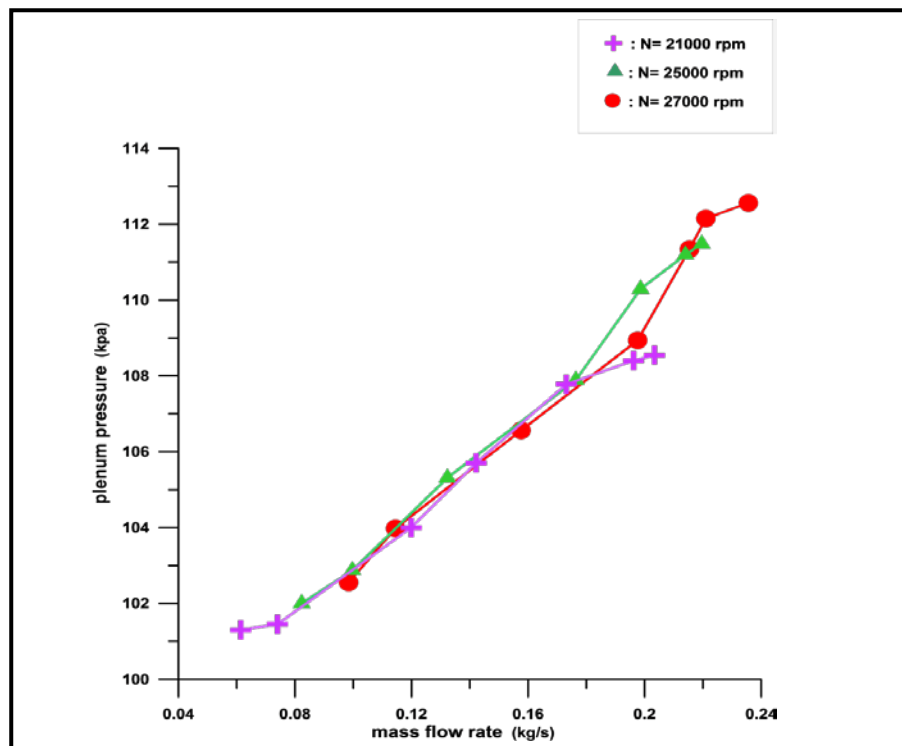


Figure (14) Mass flow rate versus plenum pressure.

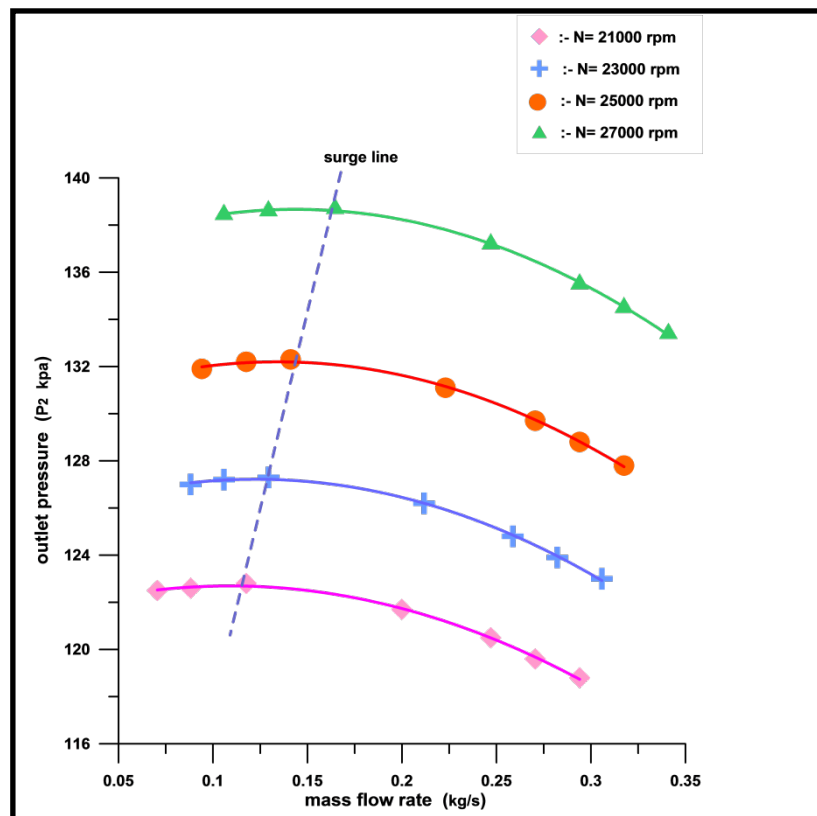


Figure (15) Mass flow rate versus outlet pressure from calculating without plenum at four rotational speeds with surge line.

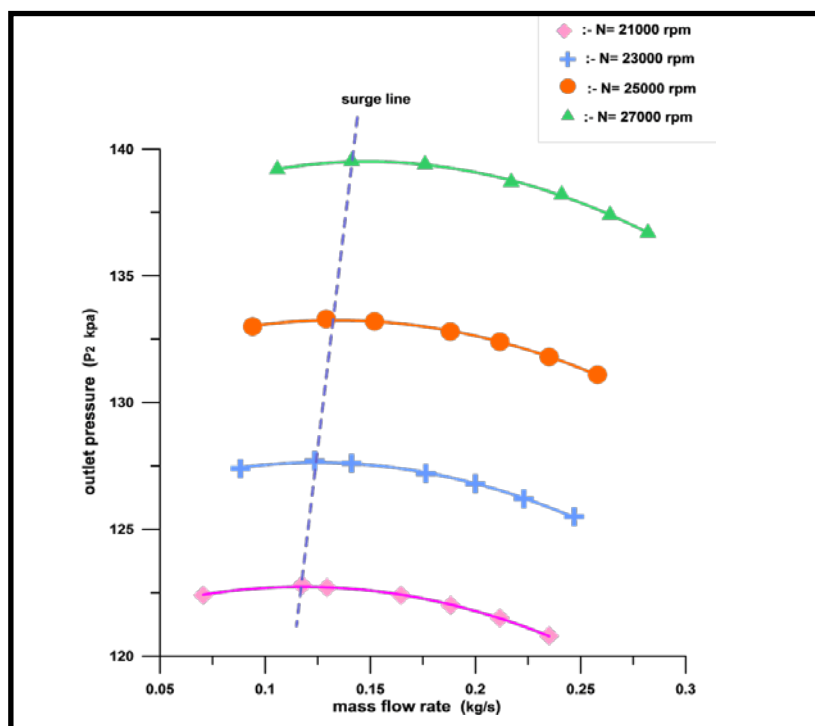


Figure (16) Mass flow rate versus outlet pressure from calculating with plenum at four rotational speeds with surge line.

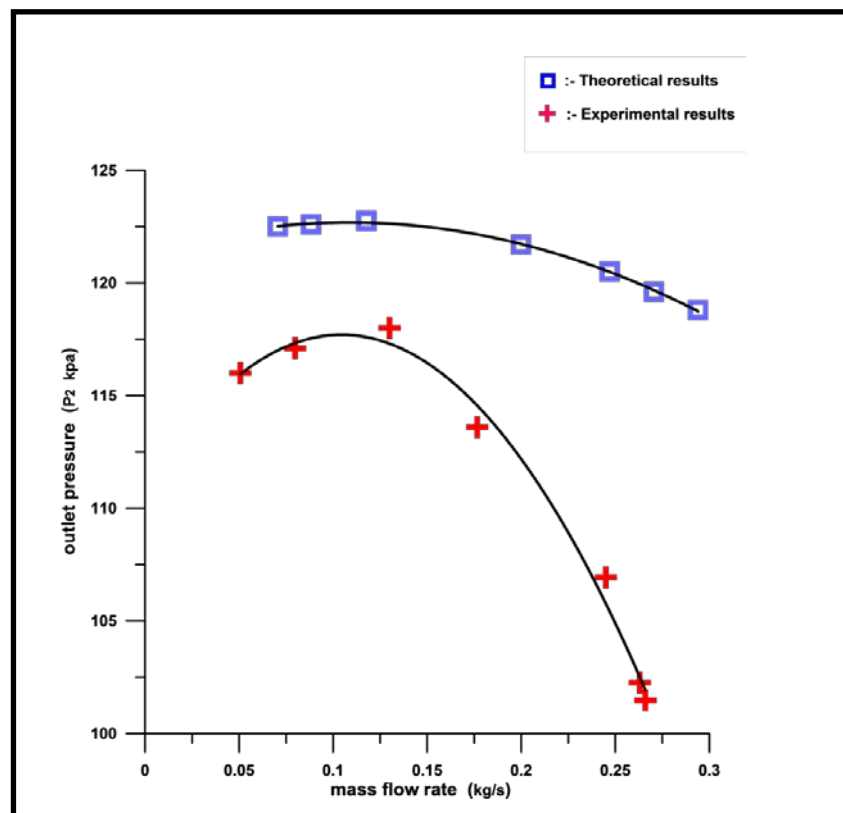


Figure (17) Mass flow rate versus outlet pressure from experimental and theoretical work without plenum at N= 21000 rpm.

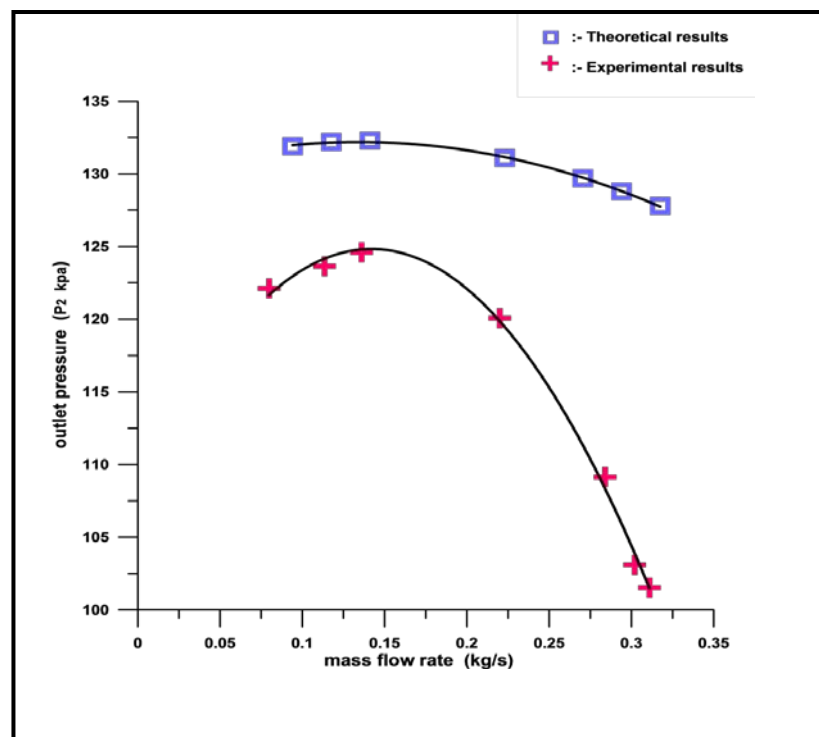


Figure (18) Mass flow rate versus outlet pressure from experimental and theoretical work without plenum at N= 25000 rpm

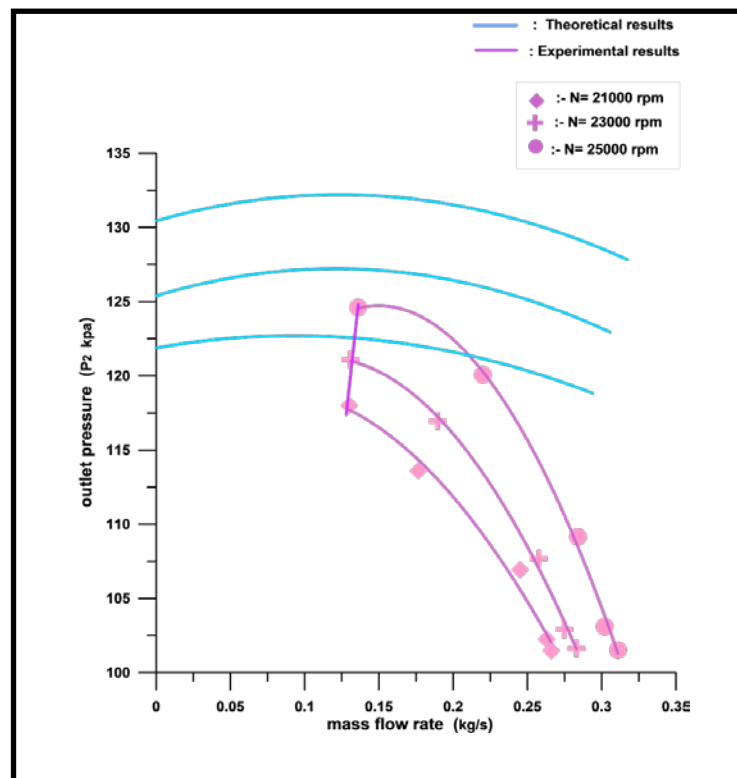


Figure (19) Mass flow rate versus outlet pressure theoretically and experimentally in three rotational speeds

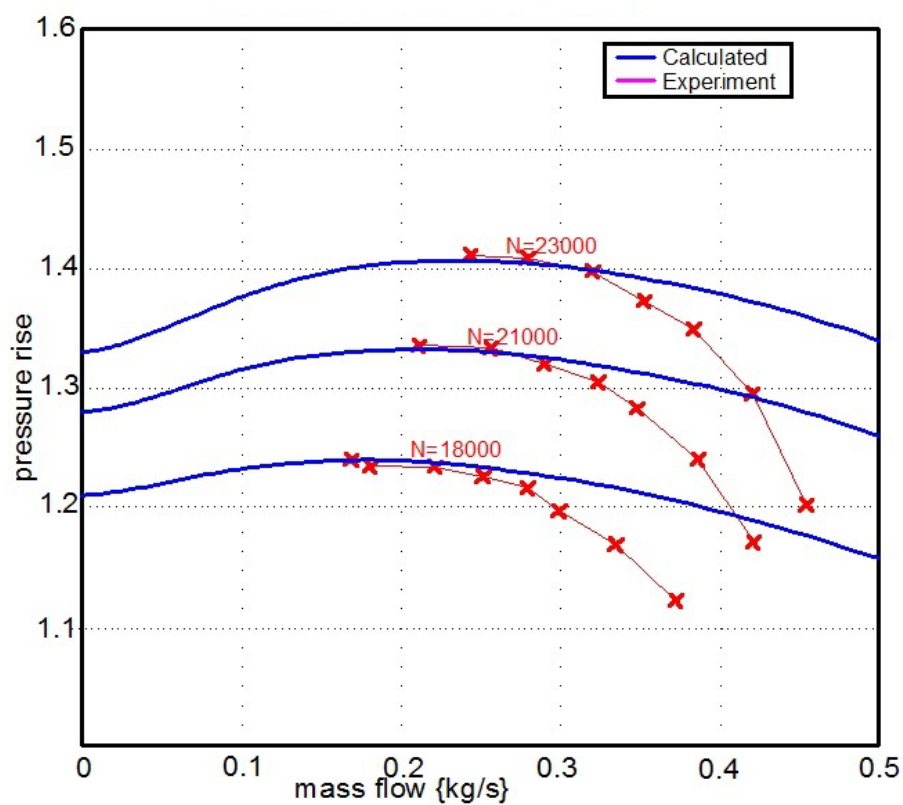


Figure (20) Mass flow rate versus pressure ratio from experimental and theoretical published results from [Gravdahl et. al. 2000] in three rotational speeds

REFERENCES :-

Alan Mironer, "Engineering fluid Mechanics", Text Book, International Student Edition, University of Lowell, 1979.

Daniel Lawrence Gysling, "Dynamic Control of Centrifugal Compressor Surge Using Tailored Structure", M.Sc. Thesis, The Pennsylvania state University, 1989.

Jan Tommy Gravdahl, "Modeling and Control of Surge and Rotating Stall in Compressors", Ph.D. thesis, Norwegian University of science and Technology, 1998.

Jan Tommy Gravdahl, Frank Willems, Bram de Jager and Olav Egeland, "Modeling for Surge Control of Centrifugal Compressors: Comparison with Experiment", Norwegian University of Science and Technology, 2000.

Jan Tommy Gravdahl, Olav Egeland and SveinOveVatland, "Active Surge Control of Centrifugal Compressors using Drive Torque", Department of Engineering Cybernetics, Norway, Proceedings of the 40th IEEE Conference on Volume 2, 2001.

Jan Tommy Gravdahl, Frank Willems, Bram de Jager and Olav Egeland, "Modeling of Surge in Free-Spool Centrifugal Compressors: Experimental Validation", Journal of Propulsion and Power, Vol. 20, No. 5, PP. 849-857, September- October, 2004.

N. A. Cumpsty, "Compressor Aerodynamics Longman", Text book, 1989.

NieChaoqun, Chen Jingyi and Chen Naixing, "Experimental Study on Active Control of Surge in a Centrifugal Compression System", International Journal of Rotating Machinery, Vol. 6, No. 5, PP. 383-392, 2000.

Raef S. Shehata, Hussein A. Abdullah and Fayez F.G. Areed, "Variable Structure Surge Control for Constant Speed Centrifugal Compressors", Vol. 17, PP. 815-833, 2009.

RashaHayderHashim, "Experimental and Theoretical Study of Surge in a Centrifugal Flow Compressor", M.Sc. Thesis, Babylon University, September, 2013.

S.L. Dixon, B. Eng., Ph. D, ''Fluid Mechanics and Thermodynamics of Turbo machinery'', Text book, Fourth Edition, University of Liverpool, 1998.

Thomas Barker Ferguson, ''The Centrifugal Compressor Stage'', Text book, London, 1963.

Torbjorn Sonstebo Grong, ''Modeling of Compressor Characteristics and Active Surge Control'', M.Sc. Thesis, Norwegian University of Science and Technology, June, 2009.